Achieving Stable Radiation Pressure Acceleration of Heavy Ions via Successive Electron Replenishment from Ionization of a High-Z Material Coating

Published in:
Physical Review Letters

Document Version:
Publisher's PDF, also known as Version of record

Queen's University Belfast - Research Portal:
Link to publication record in Queen's University Belfast Research Portal

Achieving Stable Radiation Pressure Acceleration of Heavy Ions via Successive Electron Replenishment from Ionization of a High-Z Material Coating

X. F. Shen,[1,2] B. Qiao,[1,2,3,*] H. Zhang,[1,4] S. Kar,[5] C. T. Zhou,[1,4] H. X. Chang,[1] M. Borghesi,[5] and X. T. He[1,4]

[1]*Center for Applied Physics and Technology, HEDPS, State Key Laboratory of Nuclear Physics and Technology,
and School of Physics, Peking University, Beijing 100871, China*
[2]*Collaborative Innovation Center of IFSA (CICIFSA), Shanghai Jiao Tong University, Shanghai 200240, China*
[3]*Collaborative Innovation Center of Extreme Optics, Shanxi University, Taiyuan, Shanxi 030006, China*
[4]*Institute of Applied Physics and Computational Mathematics, Beijing 100094, China*
[5]*Center for Plasma Physics, School of Mathematics and Physics, Queen's University Belfast, Belfast BT7 1NN, United Kingdom*

A method to achieve stable radiation pressure acceleration (RPA) of heavy ions from laser-irradiated ultrathin foils is proposed, where a high-Z material coating in front is used. The coated high-Z material, acting as a moving electron repository, continuously replenishes the accelerating heavy ion foil with comoving electrons in the light-sail acceleration stage due to its successive ionization under laser fields with Gaussian temporal profile. As a result, the detrimental effects such as foil deformation and electron loss induced by the Rayleigh-Taylor-like and other instabilities in RPA are significantly offset and suppressed so that stable acceleration of heavy ions are maintained. Particle-in-cell simulations show that a monoenergetic Al^{13+} beam with peak energy 3.8 GeV and particle number 10^{10} (charge $>$ 20 nC) can be obtained at intensity 10^{22} W/cm^2.

Laser-driven ion acceleration has become a highly active research field [1] due to its many prospective applications [2]. While accelerations of protons and light ions have been investigated, little has been reported on the acceleration of heavy ions. In fact, due to much heavier mass and more choices of charge to mass ratio, heavy ion beams have more advantageous applications related to nuclear science [3], high energy density physics [4], quark-gluon plasmas [5], and others. A large heavy ion accelerator, FAIR [6], is under construction. Laser-driven accelerators may offer a cheaper and smaller alternative because of orders of magnitude higher accelerating fields.

Several methods for laser-driven ion acceleration are proposed, including target normal sheath acceleration (TNSA) [7,8], radiation pressure acceleration (RPA) [9–12], and shock acceleration [13], but most of them are only favorable for protons or light ions. In the idealistic RPA, all ion species are coaccelerated, and heavy ion acceleration is not impeded by light ion contaminants [10,11], whereas this is a concern in TNSA and others. However, in realistic multidimensional RPA cases, to achieve the same energy per nucleon as protons, heavy ions undergo much more serious Rayleigh-Taylor-like (RT) instability [14,15] and, afterwards, a much worse Coulomb explosion (CE) [16]. This leads to a broad energy spectrum and a low particle number of heavy ion beams. Recently, two-dimensional (2D) particle-in-cell (PIC) simulation [17] indicates that a quasimonoenergetic Fe^{24+} beam is generated by using compound targets mixed with a Au

substrate, which, however, is limited by complicated target fabrication and rather low conversion efficiency.

In this Letter, we propose using a high-Z material coating in front of ultrathin heavy ion foils for achieving stable RPA of heavy ions by circularly polarized (CP) lasers. Because of temporally Gaussian-shaped laser fields, the high-Z coating is successively ionized from low to high charge states during acceleration, which acts as a moving electron repository providing a large number of ionized electrons. Under a strong laser ponderomotive push, these electrons can catch up with the accelerating heavy ion foil rapidly and become comoving with the latter, while the highly charged coating ions undergo CE and lag behind. This continuous replenishment of comoving electrons for the accelerating heavy ion foil offsets the detrimental effects by RT and other instabilities, suppressing deformation and CE of the foil and eventually maintaining its stable RPA. 2D and 3D PIC simulations show that a monoenergetic Al^{13+} beam with peak energy 3.8 GeV and particle number 10^{10} is obtained at 10^{22} W/cm^2.

The heavy ion acceleration equation [10–12] in RPA is

$$\frac{dv_i}{dt} = \frac{Z}{A}\frac{1}{\gamma^3}\frac{E_L^2[t - x(t)/c]}{2\pi m_p n_e l_0}\frac{c - v_i}{c + v_i}, \qquad (1)$$

where v_i is ion velocity, E_L is the laser electric field, A is the ion mass number, and Z is the charge state. Assuming the RT instability dominates initially, whose growth in the nonrelativistic regime can be estimated [14] as
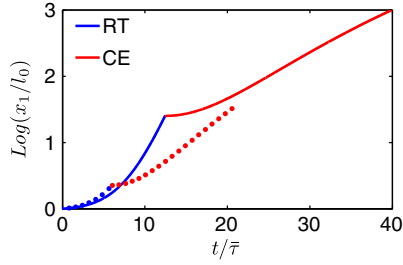
FIG. 1.   The growths of the RT instability (blue) [Eq. (2)] and Coulomb explosion (red) [Eq. (3)] with time t for protons (dashed curve) and Al^{13+} ions (solid curve), respectively, where a flat-top laser of $a = 316$ is assumed to irradiate 1.0 μm proton and Al^{13+} foils with the same electron density $n_e = 50n_c$. It shows that, to achieve the same energy/nucleon at $\gamma = 2$, the acceleration time for Al^{13+} is twice as long and the instability growth is about three times larger than for protons.

$$x_1, y_1 \propto \exp(t/\tau), \qquad \tau = \sqrt{\frac{A}{Z}} \frac{\sqrt{m_p n_e l_0 \lambda_{RT}}}{E'_L}, \qquad (2)$$

where λ_{RT} is a perturbation wavelength. Figure 1 plots the accumulated growth of instability (blue lines) obtained from Eq. (2) as $x_1 = \int_0^t (dx_1/dt)dt \approx \delta \int_0^t (\tau - t\dot{\tau})/\tau^2 \exp(t/\tau)dt$ (δ is the initial random perturbation), where τ is updated with $E'_L = E_L[(c - v_i)/(c + v_i)]^{1/2}$ by advancing the accelerating foil velocity $v_i(t)$ via Eq. (1) from $t = 0$. To achieve the same energy/nucleon, the required acceleration time [Eq. (1)] for heavy ions (such as Al^{13+}) is much longer than protons, which, as seen in Fig. 1, leads to much more serious RT instability growth.

After the RT instability significantly develops, the foil deforms and the CE dominates due to loss of electrons, leading to foil transparency and termination of RPA. Assuming the CE develops mainly in 1D, the foil thickness evolving with time can be estimated [18] as

$$l = l_0 \left(1 + \eta \frac{1}{2} \frac{Z}{A} \frac{4\pi n_e e^2}{m_p} t^2 \right), \qquad (3)$$

where η is the ratio of net positive charge. We see from Fig. 1 that, due to more serious RT instability growth, the number of the lost electrons from the heavy ion foil (η) are much larger than from the proton foil, resulting in much worse CE. Actually, this trend also occurs even for the same η after RT instability.

To suppress the above RT instability and CE in heavy ion RPA, we propose using a high-Z coating in front of ultrathin heavy ion foils, where the atomic number Z of the coating material is larger than the foil. On the one hand, as demonstrated in Refs. [19,20], a coating of high-Z material can buffer the accelerating heavy ion foil from the RT instability. More importantly, on the other hand, during the successive ionization of the high-Z coating under Gaussian laser fields, a large number of ionized electrons can be
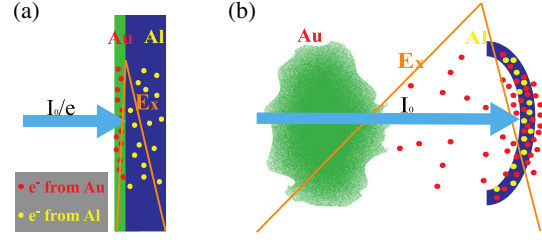

FIG. 2.   Schematic of stable heavy ion RPA via successive electron replenishment from ionization of a high-Z coating. (a) Laser fields ionize Au and Al, expelling Au electrons into Al. (b) The successive ionized electrons from the Au coating catch up and comove with the accelerating Al foil, keeping a negative gradient electric field for stable RPA.

produced and catch up with the accelerating heavy ion foil rapidly and continuously replenish the comoving electrons, the latter required for keeping stable RPA [16,20], whereas the coating itself undergoes CE and lags behind. As an example, here, we choose a Au coating in front of a thin Al foil to demonstrate the principle of our scheme, which is described as the schematic Fig. 2. Note that, recently, Bulanov *et al.* [21] discussed the maximum attainable energy of stable proton RPA in the relativistic regime, where the RT instability is much suppressed [11,14] due to the relativistic effect. However, it is hard to accelerate heavy ions to relativistic energy.

To achieve the proposed scheme, first, we need to consider the ionization dynamics in intense laser-matter interactions. The field ionization rate can be given by the Ammosov-Delone-Krainov formula [22] as $P_f = 1 - \exp(-w_z \Delta t)$ and $w_z = \omega_a \kappa^2 [(2l + 1)(l + m)!/ 2^m m!(l - m)!] \times [2^{2n^* - 2}/n^*(n^* + l)!(n^* - l - 1)!]2^{2n^* - m} F^{m+1-2n^*} \exp(-2/3F)$, where $F = |\mathbf{E}|/\kappa^3 E_a$, $\mathbf{E}$ is laser field, $E_a = m^2 e^5/h^4 = 5.1 \times 10^9$ V/cm, and $\omega_a = me^2/h^3 = 4.13 \times 10^{16}$ s^{-1}. $\kappa = \sqrt{I_Z/I_H}$ is square root of the normalized ionization potential with $I_H = 1312$ kJ/mol and $n^* = Z/\kappa$. l and m are the angular momentum and its projection along the field. The collisional ionization rate can be estimated as [23] $P_c = 1 - \exp(-n_e \sigma v_e \Delta t)$ and $\sigma = \sum_{i=1}^N a_i q_i [\ln(E/P_i)/EP_i]\{1 - b_i \exp[-c_i(E/P_i - 1)]\}$, where E is the impact electron energy, P_i is ionization potential, q_i is the number of equivalent electrons in the ith subshell. Considering intense lasers at 10^{21}–10^{22} W/cm^2, the field ionization rate from Au^{50+} to Au^{51+} is estimated as $P_f \leq 1$, while $P_c < 10^{-4}$. So the field ionization dominates [24–26], where the Au coating is ionized to be Au^{51+}. Similarly, the Al foil are estimated to be fully ionized as Al^{13+} rapidly.

Second, to balance the stability with the conversion efficiency of acceleration for Al, the areal densities of the Au coating $\sigma_{Au} = n_{e,Au} l_{Au}$ and Al foil $\sigma_{Al} = n_{e,Al} l_{Al}$ have the optimal conditions, respectively. On the one hand, $\sigma_{Al} + \sigma_{Au}$ should satisfy the optimal RPA condition [10,11]

as a whole. On the other hand, in order to not only replenish the Al foil with comoving electrons as much as possible, but also keep the loss of conversion efficiency to Au ions as low as possible, we assume that the Au coating undergoes CE rapidly at laser foot $a \sim a_0 \exp(-1)$. In other words, once the laser irradiates the target, electrons of the Au coating are completely expelled out (where the ponderomotive force should be larger than the maximum charge separation field of Au coating [11,12]) and piled up into Al foil quickly, leading to effective light-sail RPA of the whole Al foil. Therefore, the optimal conditions are

$$\sigma_{Au} = a_0 n_c \lambda / 2\pi \exp(1), \qquad (4)$$

$$\sigma_{Au} + \sigma_{Al} = a_0 n_c \lambda / \pi. \qquad (5)$$

To verify the new scheme, 2D PIC simulations are carried out with the EPOCH code [27], where the field ionization is self-consistently integrated. The simulation box (x, y) is $10 \times 12 \ \mu m$ containing 10000×1500 cells. The particle number per cell for both electrons and ions is 400 for Al foil and 200 for Au coating. The Al foil has a density of 2.7 g/cm^3, thickness 20 nm and initial charge state Al^{7+} under temperature 280 eV, and those for the Au coating are respectively 19.32 g/cm^3, 2 nm and Au^{13+}, where conditions (4) and (5) are satisfied. A CP laser with $I_0 = 10^{22}$ W/cm^2 and $\lambda = 800$ nm propagates from the left boundary at $x = -2.0 \ \mu m$ and irradiates the target at $x = 0$. The laser pulse is temporally Gaussian distributed with duration $\tau_L = 8T_0$ ($T_0 = \lambda / c$). To save computational resources and better compare with the above theory, a transversely fourth-order Gaussian spatial profile of radius $r_0 = 3 \ \mu m$ for the laser is chosen. To show the role of the

time-dependent ionization physics clearly, simulations without the ionization effect (the charge states are fixed to Al^{13+} and Au^{69+}) and without the Au coating (a 30 nm pure Al foil keeping the same total electron number) are also carried out for comparison.

In Fig. 3, electron [3(a)–3(c)], Au [3(d)–3(f)], and Al [3(g)–3(i)] density maps during acceleration are shown at $t = 4$, 13, and $19T_0$, respectively. The Al density maps for the cases without the ionization effect [3(j)–3(l)] and without the Au coating [3(m)–3(o)] are also plotted. At $t = 4T_0$ [3(a)], when the laser starts to irradiate the target, the Au coating is quickly ionized to 51+ and the Al foil is fully ionized to 13+ at the foot of the laser of $I \approx 1.35 \times 10^{21}$ W/cm^2. Afterwards, the Au ions expand in space due to CE, during which they are successively ionized to higher and higher charge states with increasing laser intensities, producing a large number of free electrons. As we expected, most of these electrons rapidly catch up with the accelerating Al foil and, then, are held in the latter by the space charge field, eventually becoming comoving electrons of the accelerating Al foil, shown in Figs. 3(b) and 4(a). From Fig. 4(a), we see that the replenished, ionized electrons from the Au coating contribute about 15% of the whole comoving electrons for acceleration of Al foil. Because of the replenishment of ionized electrons, the accelerating Al foil keeps opaque to the laser [4(c)], suppressing electron heating and deformation induced by RT and other instabilities. This further suppresses the loss of comoving electrons and, accordingly, CE, forming a positive feedback for stabilization of Al RPA. Therefore, stable RPA of the Al foil can be maintained, see Fig. 3(i), until the laser is over.
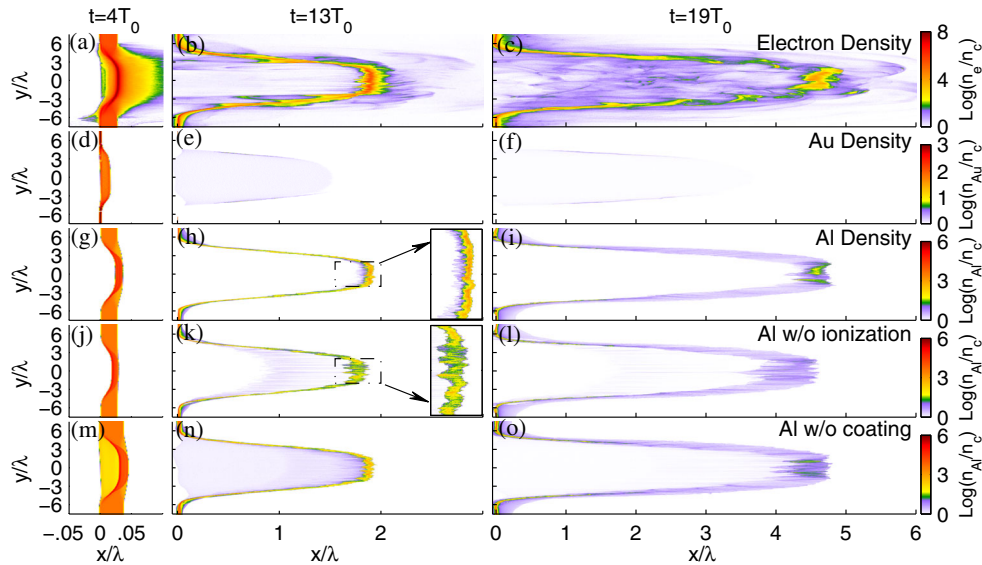

FIG. 3.   Electron density $\ln(n_e/n_c)$ (a)–(c), Au ion density $\ln(n_{Au}/n_c)$ (d)–(f), Al ion density $\ln(n_{Al}/n_c)$ (g)–(i) at $t = 4$, 13 and $19T_0$ in the acceleration of an Al foil by laser at $I_0 = 10^{22}$ W/cm^2, where a 2 nm Au coating is used. The Al ion density for the cases without ionization effect (j)–(l) and without the Au coating (m)–(o) are also plotted. Insets show zoomed density maps in the dotted-dashed boxes, which indicates the seriousness of the RT instability.
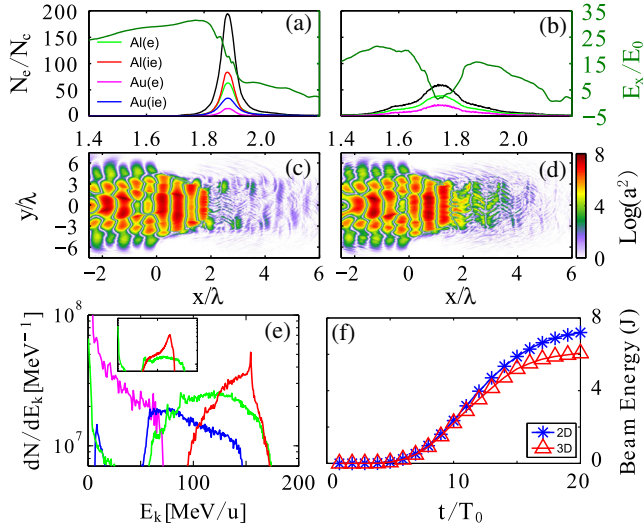
FIG. 4. The longitudinal profiles of electron density n_e/n_c and electric field E_x (green line) at $t = 13T_0$ with (a) and without (b) ionization in simulation of Fig. 3. In (a), the cyan, red, magenta, and blue lines represent the initial electrons from Al ions, the ionized electrons from Al, the initial electrons from Au, and the ionized electrons from Au, respectively, while the black line shows the sum of all electrons. In (b), the cyan and magenta lines correspond to the electrons from Al and Au, respectively, and the black line shows their sum. (c) and (d) Laser intensity distributions with and without ionization. (e) The energy spectra of Al^{13+} within $|y| < 2$ μm by our scheme (red), without ionization (blue), and without Au coating (green) at $t = 20T_0$. The magenta line corresponds to Au ions, but with dN/dE_k multiplied by 5 times. (f) The total energy of the Al^{13+} beam increasing with time for the 2D (blue star) and 3D (red triangle) simulations. Inset of (e) shows the Al^{13+} spectra for the cases of, respectively, with (red line) and without (green line) Au coating by using a Gaussian and elliptically polarized laser pulse with ellipticity $|E_y|/|E_z| = 0.8$, where other parameters are the same as here.

If the ionization effect is not considered, as shown in Fig. 4(b), the total comoving electron density in the accelerating Al foil drops by three times lower, leading to transparency [4(d)] and serious instabilities [3(k), comparing inset with 3(h)] of the latter. Therefore, RPA of Al^{13+} terminates quickly [3(l)]. Similarly, without Au coating, no replenishment of electrons occurs, RPA of Al^{13+} also becomes unstable quickly, shown in Fig. 3(o).

Figure 4(e) plots the final energy spectra of Al^{13+} at $t = 20T_0$ for different cases when the laser is over. By using our scheme, a quasimonoenergetic Al beam with peak energy 150 MeV/u (4.0 GeV) and energy spread of 25% is produced. The particle number with energy ≥ 100 MeV/u is about 10^{10} (charge 20 nC) and the total beam energy is about 7J [4(f)], at least one order larger than Refs. [17,24]. However, for both cases, without ionization and without Au coating, the energy spectra are much broadened due to premature termination of RPA and CE, see the blue and green lines in 4(e). These clearly imply the vital importance of the time-dependent ionization physics in our scheme, without which only the buffering effect of high-Z species against the RT instabilities [17,19,20] is insufficient to maintain stable RPA. Note that, in experiments, the required contrast above 10^{10} at picosecond pedestal duration can be achieved now [28,29]. Circular polarization of lasers can be obtained by using a mica crystal with a $\lambda/4$ wave plate [30]; however, it may not be perfect. Considering a more realistic Gaussian and elliptically polarized laser with $|E_y|/|E_z| = 0.8$, we plot the Al energy spectra for both with and without Au coating cases in the inset of Fig. 4(e). It clearly shows that the improvement in ion energy spectra is still substantial by using our scheme.

Large-scale 3D PIC simulations are also carried out. The simulation setup keeps almost the same as that in 2D except the particle number per cell is reduced to be 64 for Al and 100 for Au. The Al^{13+} densities at $t = 20T_0$ for the cases with and without ionization are shown in Figs. 5(a) and 5(b). Figure 5(c) shows their corresponding energy spectra. A quasimonoenergetic Al^{13+} beam with a peak energy of 140 MeV/u is also obtained, which is much better than that for the case without ionization. Thus, we conclude that 3D effect does not qualitatively impact our scheme. The slight decrease of ion energy in 3D simulation, with respect to 2D, may be attributed to the smaller reflectivity of the accelerating foil as $R \simeq \sigma^2/(1 + \sigma^2)$ [12] and resultantly weaker radiation pressure $P_{rad} = 2RI/c$ in 3D, where $\sigma = \pi(n_e/n_c)(l/\lambda)$ decreases faster due to heavier electron loss in 3D. Here, the transverse expansion of the foil during acceleration is small, which is different from that in Refs. [31].
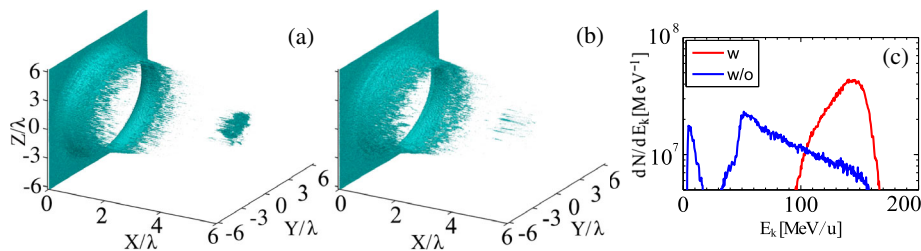

FIG. 5. 3D PIC simulation results: the Al^{13+} density isosurface for $n = 3n_c$ with (a) and without (b) the ionization effect at $t = 20T_0$. (c) The corresponding energy spectra of Al^{13+} within $r < 2$ μm with (red curve) and without (blue curve) the ionization effect.

In conclusion, a novel scheme for achieving stable RPA of heavy ions from laser-irradiated ultrathin foils is proposed, where a high-Z material coating in front of the foil plays a key role as a moving electron repository, successively replenishing heavy ion acceleration with comoving electrons.

[*]bqiao@pku.edu.cn

[1] A. Macchi, M. Borghesi, and M. Passoni, Rev. Mod. Phys. **85**, 751 (2013).

[2] H. Daido, M. Nishiuchi, and A. S. Pirozhkov, Rep. Prog. Phys. **75**, 056401 (2012).

[3] F. N. Beg *et al.*, Appl. Phys. Lett. **80**, 3009 (2002); P. McKenna *et al.*, Phys. Rev. E **70**, 036405 (2004).

[4] N. A. Tahir *et al.*, Phys. Rev. Lett. **95**, 035001 (2005).

[5] G. Agakishiev *et al.* (STAR Collaboration), Phys. Rev. Lett. **108**, 072301 (2012).

[6] W. F. Henning, Nucl. Instrum. Methods Phys. Res. **214**, 211 (2004).

[7] S. C. Wilks, A. B. Langdon, T. E. Cowan, M. Roth, M. Singh, S. Hatchett, M. H. Key, D. Pennington, A. MacKinnon, and R. A. Snavely, Phys. Plasmas **8**, 542 (2001).

[8] H. Schwoerer, S. Pfotenhauer, O. Jäckel, K.-U. Amthor, B. Liesfeld, W. Ziegler, R. Sauerbrey, K. W. D. Ledingham, and T. Esirkepov, Nature (London) **439**, 445 (2006).

[9] A. Macchi, F. Cattani, T. V. Liseykina, and F. Cornolti, Phys. Rev. Lett. **94**, 165003 (2005).

[10] A. P. L. Robinson, M. Zepf, S. Kar, R. G. Evans, and C. Bellei, New J. Phys. **10**, 013021 (2008).

[11] B. Qiao, M. Zepf, M. Borghesi, and M. Geissler, Phys. Rev. Lett. **102**, 145002 (2009).

[12] A. Macchi, S. Veghini, and F. Pegoraro, Phys. Rev. Lett. **103**, 085003 (2009).

[13] F. Fiuza, A. Stockem, E. Boella, R. A. Fonseca, L. O. Silva, D. Haberberger, S. Tochitsky, C. Gong, W. B. Mori, and C. Joshi, Phys. Rev. Lett. **109**, 215001 (2012).

[14] F. Pegoraro and S. V. Bulanov, Phys. Rev. Lett. **99**, 065002 (2007).

[15] D. Wu, C. Y. Zheng, B. Qiao, C. T. Zhou, X. Q. Yan, M. Y. Yu, and X. T. He, Phys. Rev. E **90**, 023101 (2014).

[16] B. Qiao, M. Zepf, P. Gibbon, M. Borghesi, B. Dromey, S. Kar, J. Schreiber, and M. Geissler, Phys. Plasmas **18**, 043102 (2011); B. Qiao, S. Kar, M. Geissler, P. Gibbon, M. Zepf, and M. Borghesi, Phys. Rev. Lett. **108**, 115002 (2012).

[17] A. V. Korzhimanov, E. S. Efimenko, S. V. Golubev, and A. V. Kim, Phys. Rev. Lett. **109**, 245008 (2012).

[18] E. Fourkal, I. Velchev, and C.-M. Ma, Phys. Rev. E **71**, 036412 (2005).

[19] T. P. Yu, A. Pukhov, G. Shvets, and M. Chen, Phys. Rev. Lett. **105**, 065002 (2010).

[20] B. Qiao, M. Zepf, M. Borghesi, B. Dromey, M. Geissler, A. Karmakar, and P. Gibbon, Phys. Rev. Lett. **105**, 155002 (2010).

[21] S. S. Bulanov, E. Esarey, C. B. Schroeder, S. V. Bulanov, T. Zh. Esirkepov, M. Kando, F. Pegoraro, and W. P. Leemans, Phys. Rev. Lett. **114**, 105003 (2015).

[22] V. S. Popov, Phys. Usp. **47**, 855 (2004).

[23] W. Lotz, Z. Phys. **206**, 205 (1967).

[24] D. Wu, B. Qiao, C. McGuffey, X. T. He, and F. N. Beg, Phys. Plasmas **21**, 123118 (2014).

[25] A. J. Kemp, R. E. W. Pfund, and J. Meyer-ter-Vehn, Phys. Plasmas **11**, 5648 (2004).

[26] Y. Sentoku and A. J. Kemp, J. Comput. Phys. **227**, 6846 (2008).

[27] T. D. Arber *et al.*, Plasma Phys. Controlled Fusion **57**, 113001 (2015).

[28] B. Dromey, S. Kar, M. Zepf, and P. Foster, Rev. Sci. Instrum. **75**, 645 (2004).

[29] F. Tavella, A. Marcinkevicius, and F. Krausz, Opt. Express **14**, 12822 (2006).

[30] A. Henig *et al.*, Phys. Rev. Lett. **103**, 245003 (2009).

[31] S. V. Bulanov, E. Y. Echina, T. Z. Esirkepov, I. N. Inovenkov, M. Kando, F. Pegoraro, and G. Korn, Phys. Rev. Lett. **104**, 135003 (2010); M. Tamburini, T. V. Liseykina, F. Pegoraro, and A. Macchi, Phys. Rev. E **85**, 016407 (2012).